SELF-FOCUSING OF RAYLEIGH WAVES: SIMULATION AND EXPERIMENT

W.A.K. Deutsch, A.Cheng, J.D. Achenbach

Center for Quality Engineering and Failure Prevention
Northwestern University, Evanston, IL 60208-3020

INTRODUCTION

In earlier work [1,2] a simple idea for self-focusing of a linear array has been used for Rayleigh and Lamb waves. The self-focusing procedure automatically moves the focal region of the array towards the defect that produces the largest backscattered signal by adjusting the excitation times of the elements of the array. Experimental results demonstrate the ability to self-focus Rayleigh waves and Lamb waves on defects in thick slabs and thin sheets. The aim of this paper is to supplement the experimental results with a measurement model of the self-focusing of surface waves. A model for the surface wave generated by a single element of the linear array has been developed. The field generated by the entire array has been simulated by using superposition.

SELF-FOCUSING ULTRASONICS

Conventional NDT often uses a focused transducer to increase the amplitude of ultrasonic signals [3]. Since focused transducers have a fixed focal point, mechanical movement of the transducer is generally required to focus on a defect, resulting in long inspection times and extra expenses for a scanning device. A phased array technique allows one to electronically move the focal point without mechanically moving the transducer itself [4,5].

The self-focusing procedure discussed in this paper automatically places the focal point on the defect producing the biggest ultrasonic reflection within the focal range (Figure 1). The procedure works as follows: First a center element of the transducer array is excited (Figure 1a) and the defect scatters the incident wave. All transducer array elements collect the backscattered wave (Figure 1b). The arrival time for each element is dependent on the path length between the defect and the individual element. After collecting the backscattered wave with all elements a cross-correlation technique is used to determine the time-of-flight differences (Figure 1c). The time shifts determined by the cross-correlation are the time delays for reception. The element which received the signal last (i.e. has the longest path) has the biggest time delay. In transmission focusing, the waves sent out by all elements arrive at the defect at the same time (Figure 1d). The excitation times for transmission focusing are obtained by reversing the receiving time delays. The element with the longest path is fired first. Transmission focusing ensures that the sound energy at the defect location is much larger compared to a conventional transducer with the same

Review of Progress in Quantitative Nondestructive Evaluation, Vol. 17
Edited by D.O. Thompson and D.E. Chimenti,, Plenum Press, New York, 1998

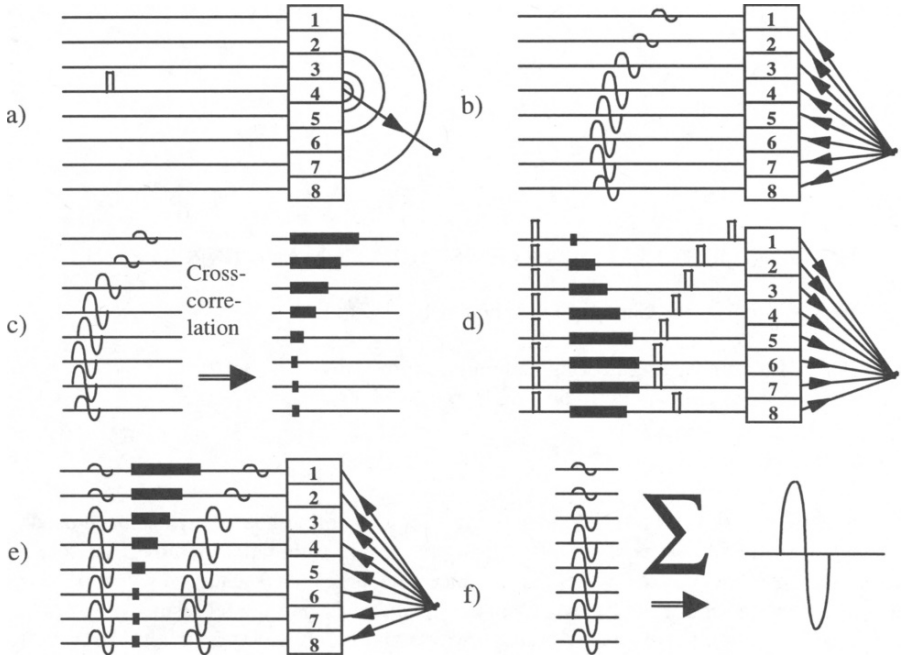

Figure 1. Steps of the self-focusing procedure a) firing center element, b) receiving with all elements, c) determination of time-of-flight differences, d) transmission focusing, e) reception focusing, and f) superposition gives focused signal.

aperture. After scattering of the focused wave by the defect (Figure 1e), reception focusing uses the previously determined receiving time delays to align the signals received by all elements. After the alignment, the positive and negative half-waves of the ultrasonic signals will match (Figure 1f). A superposition of all shifted signals then leads to constructive interference and produces the focused signal.

SELF-FOCUSING SYSTEM

The self-focusing system consists of eight identical channels. Each channel drives one element of the transducer array. The center frequency of the linear array was 5 MHz and an acrylic wedge was employed to couple the array to the surface of the specimen. The wedge angle was optimized for Rayleigh wave generation. The cost of the system was minimized by using mostly standard hardware components. Only the delay electronics which were necessary to produce the time delays for transmission focusing and the transducer array were specially built at Northwestern University. Using this system, self-focusing of Lamb waves and Rayleigh waves has been carried out for aluminum specimens with artificial defects [1,2].

THEORETICAL DISPLACEMENTS OF A NON-PLANE SURFACE WAVE

Usually, only the case of plane harmonic surface waves is discussed in the literature [6]. Self-focusing with a linear phased array does not produce a plane wave. Therefore, the

conditions for the surface wave displacement without the restriction on plane waves will be presented here.

A solid half-space referred to Cartesian coordinates is considered (Figure 2a). The half-space is defined by $x_3 \geq 0$, and the surface of the solid is given by the x_1-x_2 plane. Assuming a traction-free surface and an exponential decay with respect to x_3 for all field components leads to Equation (1) for the normal displacement

$$u_3(x_1, x_2, x_3, t) = \left[\left(1 - \frac{c_R^2}{2c_T^2} \right) e^{-ax_3} - e^{-bx_3} \right] \Gamma(x_1, x_2) e^{i\omega t}, \tag{1}$$

where c_R and c_T are the wave speeds for the Rayleigh wave and the transverse wave, respectively [7,8]. The constants a and b are defined by

$$a = k_R \sqrt{1 - \frac{c_R^2}{c_L^2}} \quad \text{and} \quad b = k_R \sqrt{1 - \frac{c_R^2}{c_T^2}}, \tag{2}$$

where c_L is the speed of the longitudinal wave, and $k_R = \omega/c_R$ is the wave number for a surface wave. It can be shown that the function $\Gamma(x_1,x_2)$ has to satisfy the Helmholtz equation

$$\Delta\Gamma(x_1, x_2) + k_R^2 \Gamma(x_1, x_2) = 0, \tag{3}$$

where Δ is the two-dimensional Laplacian.

APPROXIMATE TIME HARMONIC SOLUTION FOR THE SURFACE DISPLACEMENT

The transducer wedge is positioned so that the main propagation direction is x_1 (Figure 2a). The Rayleigh wave decays exponentially with respect to x_3 into the depth of the half space according to Equation (1). To obtain an approximate solution for a single array element, polar coordinates for the specimen surface are introduced (Figure 2b). The radius r is the distance from the origin, and the angle φ is the deviation from the x_1-axis.

It is expected that sound energy transmitted by a single array element (e.g. element #4 in Figure 2c) will only be radiated within an opening angle $\Delta\varphi$. This behavior can be approximated by a Gaussian distribution

$$Gauss(\varphi) = e^{-\frac{\varphi^2}{2\hat{\varphi}^2}}, \tag{4}$$

where the angle $\hat{\varphi}$ represents the width of the Gaussian. The width $\hat{\varphi}$ corresponds to half of the opening angle $\Delta\varphi$ of the array element. This assumption will later be validated by experimental results. The radial dependence was expressed as an asymptotic expansion which is valid for the far field of the individual array element. Satisfying Equation (3) and keeping only the first-order term of the asymptotic expansion leads to the following expression for the normal displacement at $x_3=0$ transmitted by a single array element

$$u_3(r, \varphi, t) = A \frac{e^{-\frac{\varphi^2}{2\hat{\varphi}^2}}}{\sqrt{k_R r}} e^{i(\omega t - k_R r)}, \tag{5}$$

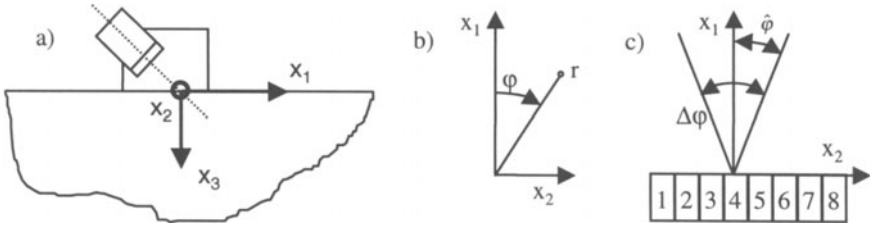

Figure 2. Self-focusing array located at the origin of the solid half space, a) side view, b) top view shows relationship between Cartesian and polar coordinates, and c) top view of the array with element #4 located at the origin of the half space.

where A is a constant amplitude factor. The fraction in Equation (5) describes the envelope of the displacement u_3. The remainder is the standard expression for a harmonic wave, travelling away from the origin with the surface wave speed c_R.

TRANSIENT SOLUTION FOR A TRAVELLING WAVE PULSE

The approximate solution stated in the previous section is valid for harmonic surface waves. A surface wave generated by an array element is a travelling pulse, which consists of a multitude of harmonics. A linear time-invariant system (Figure 3a) will be used to simulate the transient surface displacement generated by a single transducer element of the self-focusing array.

Surface displacement measurements have shown that the considered system is nondispersive. The shape of the wave pulse is independent of the position, but the peak-to-peak amplitude does change according to Equation (5). The output signal will be delayed by $\Delta t = (r-r_0)/c_R$ with respect to the input signal. This delay is caused by the radial path difference between the reference point P_0 and the observation point P (Figure 3b). This leads to the expression for the system transfer function

$$H(\omega) = \frac{\sqrt{k_R r_0}}{e^{-\frac{\varphi_0^2}{2\hat{\varphi}^2}}} \frac{e^{-\frac{\varphi^2}{2\hat{\varphi}^2}}}{\sqrt{k_R r}} e^{i\omega\frac{r-r_0}{c_R}} = C \frac{e^{-\frac{\varphi^2}{2\hat{\varphi}^2}}}{\sqrt{k_R r}} e^{i\omega\Delta t}, \tag{6}$$

where the constant C is dependent on the coordinates r_0 and φ_0 of the reference point. The corresponding impulse response in the time domain is given by

$$h(t) = C \frac{e^{-\frac{\varphi^2}{2\hat{\varphi}^2}}}{\sqrt{k_R r}} \delta(t-\Delta t). \tag{7}$$

The input signal $u_{3P0}(t)$ of the system is a measured waveform in order to represent the shape of the propagating wave (Figure 4). The signal was obtained with a heterodyne laser interferometer at the location P_0 (Figure 3b). In principle, the reference point can be located at an arbitrary position because the shape of the waveform is not dependent on the position, but some restrictions apply. The reference point P_0 has to be within the steering range of the self-focusing array ($\varphi_0 \le \hat{\varphi}$) and it has to be in the far field of a single array element, because the model is only valid for the far field.

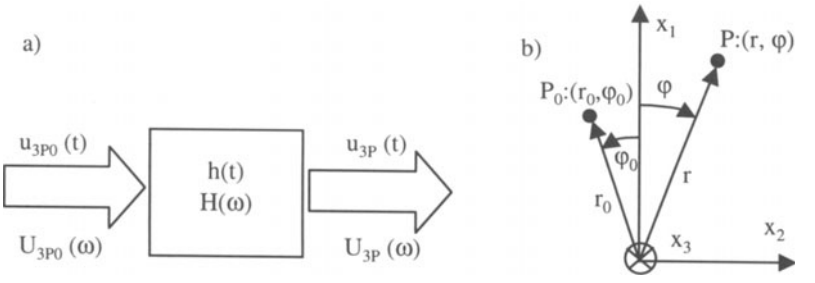

Figure 3. Simulation of the surface wave displacement, a) represented as a linear time-invariant system, and b) position of reference point P_0 and the observation point P.

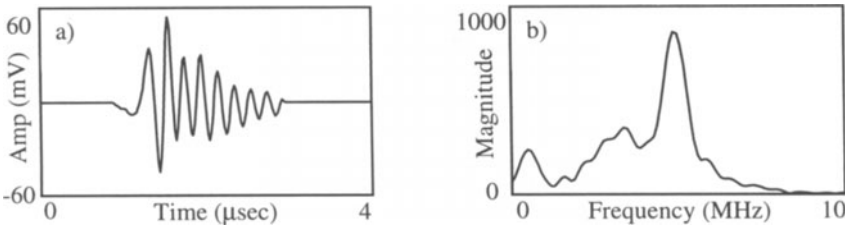

Figure 4. Measured surface wave at reference point P_0, a) time domain data, and b) spectrum.

The output signal $u_{3P}(t)$ is then given by the convolution of the impulse response h(t) and the input signal. The convolution of an input signal with a shifted delta pulse will result in a time shift of the original input. Therefore, the output signal can be calculated as

$$u_{3P}(r,\varphi,t) = \int_{-\infty}^{\infty} u_{3P0}(\tau)\; h(t-\tau)\, d\tau = C\frac{e^{-\frac{\varphi^2}{2\hat{\varphi}^2}}}{\sqrt{k_R r}} u_{3P0}(t-\Delta t)\,. \tag{8}$$

MEASURED SURFACE DISPLACEMENT OF ONE ARRAY ELELEMT

The surface displacement produced by a single array element was measured with a Heterodyne laser interferometer [9] for various positions on the specimen (Figure 5a). Each element shows similar properties and results for element #4 will be presented in this section. The position of the measurement point is defined by the radius r and the angle φ. First a measurement was taken along the center axis with fixed angle φ=0. Next the displacement was recorded at various angles but with a fixed radius r_i, where i=1..3 (Figure 5b).

The result along the center axis shows that the amplitude decays with respect to the radius and is proportional to $1/\sqrt{r}$ (Figure 6a). The result matches with the radial dependence in Equation (8). Figure (6b) shows that a Gaussian distribution (Equation 4) is a reasonable assumption for the angular dependence of the sound field. The width $\hat{\varphi}$ was determined with a best fit in the least-square sense, minimizing the error between measured data and the Gaussian distribution. The value for $\hat{\varphi}$ was determined to be approximately

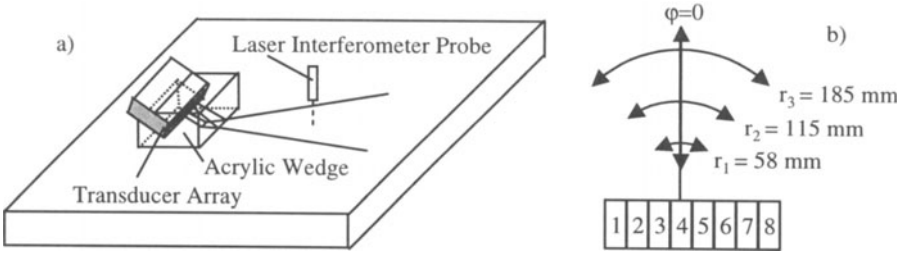

Figure 5. Measurement of the surface displacement produced by a single array element (#4), a) setup of the experiment, and b) positions for which the surface displacement was measured.

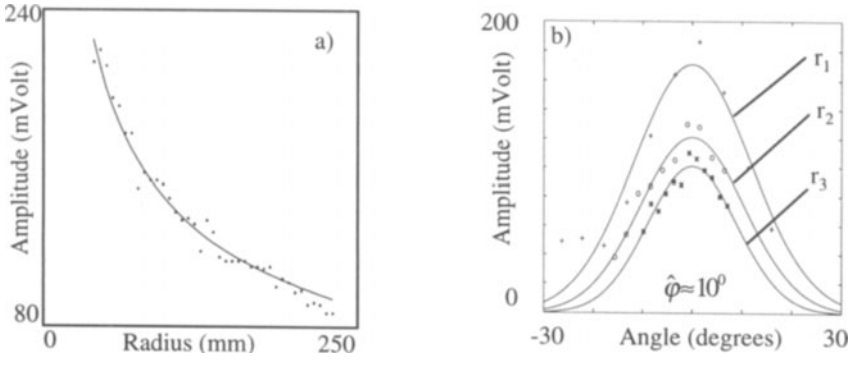

Figure 6. Measurement results of the surface displacement for a single array element, a) result along the center axis, and b) result for varied angle but fixed radius r_i.

10 degrees for all three radii, which means that sound energy is radiated within an angular range $\Delta\varphi = 2\hat{\varphi}$ of 20 degrees.

DISPLACEMENTS PRODUCED BY A SELF-FOCUSING SURFACE WAVE ARRAY

The final step is to determine the displacement produced by a linear array of n elements. This is accomplished by superposing the displacements $u_{3P,n}(r,\varphi,t)$ for all elements (Equation 8). All elements are positioned along the x_2-axis, and the element spacing is 3.5 mm. Furthermore, each element is excited with a different time delay T_n. The time delays for the self-focusing array are determined with the self-focusing procedure. This procedure is based on ultrasonic reflections from a defect, which is insonified by an initial unfocused transmission by the center element of the array. For the simulation an arbitrary focal point P_F of the array has to be chosen. The necessary time delays T_n for focusing on P_F can be calculated by

$$T_n = \frac{r_F}{c_R}\left\{1-\sqrt{1+\left(\frac{nd}{r_F}\right)^2-2\left(\frac{nd}{r_F}\right)\sin\varphi}\right\}, \tag{9}$$

where n represents the element number, d is the element spacing, and r_F is the distance of P_F from the origin [4]. The steering angle φ is the deviation from the x_1-axis. To apply this formula, one element has to be located at the origin of the half-space. The index n then takes positive and negative values, and the element at the origin is indicated with n=0. The displacement of a self-focusing surface wave array is then given by

$$u_{3ARRAY}(\mathbf{r},t)=\sum_{n=1}^{8}u_{3P,n}(\mathbf{r}-\mathbf{r_n},t-T_n), \tag{10}$$

where the vector $\mathbf{r_n}$ defines the position of element n.

SIMULATION RESULTS

Using the simulation developed in the previous sections, a MatLab-based simulation software has been implemented. Various parameters ensure flexibility of the simulation software. The number of pixels per millimeter can be chosen in order to obtain a reasonable compromise on accuracy and computing time. The number of phased array elements and their spacing were chosen in order to match the experimental setup. Figure 7 shows the simulation result for on-axis focusing. The focal point was chosen to be x_1= 20 mm and x_2= 0 mm. The figure shows a snapshot of the u_3 displacement as a function of x_1 and x_2 for a specific time, namely, the time that the maximum amplitude of the pulse passes through the focal point. A high concentration of sound energy at the focal point is observed. Similarly, focusing can be simulated for any focal point which is within the steering range. The steering range of a phased array can be roughly estimated by the opening angle Δφ of a single element. The opening angle has been measured and the value is 20 degrees.

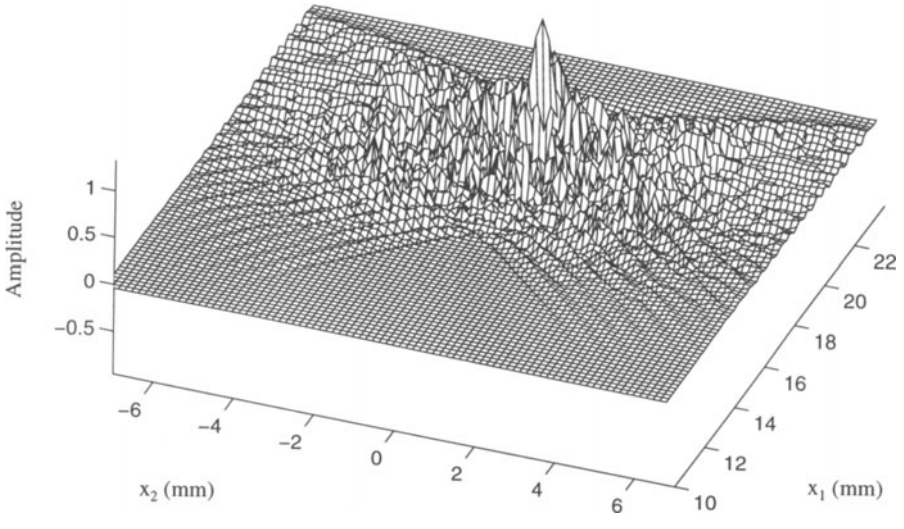

Figure 7. Simulated surface displacement for on-axis focusing.

CONCLUSION

A simple model for the surface displacement produced by a linear self-focusing array has been obtained. Simulation software has been implemented to visualize the focusing effects. The simulation shows the high concentration of sound energy at the focal point.

ACKNOWLEDGEMENTS

This work was carried out on a project funded by the Air Force Office of Scientific Research (Contract No. F 49620-93-1-0257) and by the Federal Aviation Administration (95G32).

REFERENCES

1. Deutsch, W.A.K., Cheng, A. and Achenbach, J.D.: Self-Focusing Surface Wave Array, Review of Progress in QNDE, ed. by Thompson, D.O. and Chimenti, D.A., Plenum Press, New York, Vol. 16, pp. 2077-2084, 1997
2. Deutsch, W.A.K., Cheng, A. and Achenbach, J.D.: Self-Focusing of Rayleigh Waves and Lamb Waves with a Linear Phased Array, Research in NDE, Vol. 9, pp. 81-95, 1997
3. Krautkrämer, J. and Krautkrämer, H., Ultrasonic Testing of Materials, 4th Edition, Springer Verlag, Berlin, 1990
4. von Ramm, O.T. and Smith, S.W., Beamsteering with Linear Arrays, IEEE Trans. Biomed. Eng., Vol. BME-30, pp. 438-452, 1983
5. Beardsley, B., Peterson, M. and Achenbach, J.D., A Simple Scheme for Self-Focusing of an Array, J. Nondestr. Eval, Vol. 14 (4), pp. 169-179, 1995
6. Viktorov, I.A.: Rayleigh and Lamb Waves (Physical Theory and Applications), New York, Plenum Press, pp. 96-103, 1967
7. Achenbach, J.D.: Wave Propagation in Elastic Solids, North Holland, Amsterdam / New York, 1973
8. Knowles, J.K.: A Note on Elastic Surface Waves, Journal of Geophysical Research, Vol. 71, pp. 5480-5481, 1966
9. Pouet, B.; Ing, R.K.; Krishnaswamy, S.; Royer, D.: Adaptive Heterodyne Interferometer for Ultrasonic NDE, these proceedings